A&A 604, A107 (2017)
DOI: 10.1051/0004-6361/201730679

Astronomy & Astrophysics

Distances of cataclysmic variables and related objects derived from *Gaia* Data Release 1

Gavin Ramsay[1], Matthias R. Schreiber[2], Boris T. Gänsicke[3], and Peter J. Wheatley[3]

[1] Armagh Observatory and Planetarium, College Hill, Armagh, BT61 9DG, UK
e-mail: gar@arm.ac.uk
[2] Instituto de Física y Astronomía, Universidad de Valparaíso, Valparaíso, Chile
[3] Department of Physics, University of Warwick, Coventry CV4 7AL, UK

Received 22 February 2017 / Accepted 2 April 2017

ABSTRACT

We consider the parallaxes of sixteen cataclysmic variables and related objects that are included in the TGAS catalogue, which is part of the *Gaia* first data release, and compared these with previous parallax measurements. The parallax of the dwarf nova SS Cyg is consistent with the parallax determination made using the VLBI, but with only one of the analyses of the HST Fine Guidance Sensor (FGS) observations of this system. In contrast, the *Gaia* parallaxes of V603 Aql and RR Pic are broadly consistent, but less precise than the HST/FGS measurements. The *Gaia* parallaxes of IX Vel, V3885 Sgr, and AE Aqr are consistent with, but much more accurate than the HIPPARCOS measurements. We took the derived *Gaia* distances and find that absolute magnitudes of outbursting systems show a weak correlation with orbital period. For systems with measured X-ray fluxes we find that the X-ray luminosity is a clear indicator of whether the accretion disc is in the hot and ionised or cool and neutral state. We also find evidence for the X-ray emission of both low and high state discs correlating with orbital period, and hence the long-term average accretion rate. The inferred mass accretion rates for the nova-like variables and dwarf novae are compared with the critical mass accretion rate predicted by the Disc Instability Model. While we found agreement to be good for most systems there appears to be some uncertainty in the system parameters of SS Cyg. Our results illustrate how future *Gaia* data releases will be an extremely valuable resource in mapping the evolution of cataclysmic variables.

Key words. stars: dwarf novae – stars: distances – accretion, accretion disks

1. Introduction

Cataclysmic variables (CVs) are binary stars containing a white dwarf that is accreting material from a red dwarf secondary (see Warner 1995, for a comprehensive review). Their observed characteristics are inhomogeneous and are largely set by the orbital period, the masses of the two stars, and the magnetic field strength of the white dwarf. Angular momentum is gradually lost from the system through magnetic braking and gravitational wave emission resulting in a shrinking orbital separation between the stellar components, reaching a minimum orbital period, $P_{\rm orb} \simeq 80$ min (see Gänsicke et al. 2009; Knigge et al. 2011).

CVs fall into two broad categories: in those with weakly or non-magnetic white dwarfs the mass transfer proceeds through an accretion disc, whereas strong magnetic white dwarfs disrupt the disc (the DQ Her stars or Intermediate Polars), or prevent its formation altogether (the AM Her stars or Polars). Among the non-magnetic systems, the long-term variability further divides CV subtypes based on the mass loss rate of the companion star. Nova-like (NL) CVs have mostly $P_{\rm orb} > 3$ h, high mass transfer rates and stable discs which are hotter than the ionisation threshold of hydrogen. The NL systems include various sub-classes, including the UX UMa systems with steady bright discs, and the VY Scl systems which undergo low states when the brightness drops by two to five magnitudes. These episodes are thought to be due to a reduction (or cessation) in the mass transfer rate. The dwarf novae (DN) spend most of the time in a faint quiescent state, in which their discs are cool and neutral. Occasionally, every few weeks to years, they show outbursts, during which the disc is heated above the ionisation temperature of hydrogen and the accretion rate through the disc increases dramatically. A subset of DN (SU UMa systems, generally with $P_{\rm orb} \lesssim 2$ h) additionally show longer and brighter superoutbursts that typically occur every few months. Other DN subsets (U Gem and Z Cam systems) typically have $P_{\rm orb} \gtrsim 3$ h and also show outbursts. In addition the Z Cam systems show "standstills" in their light curve and are thought to be on the boundary between NL variables with their hot stable discs, and DN with their unstable discs.

It is now widely accepted that outbursts occur due to instabilities in the accretion disc, with some role for irradiation of the secondary influencing the mass transfer rate. This Disc Instability Model (DIM) and can explain many (but not all) of the features seen in DN and other outbursting systems (see e.g. Hōshi 1979; Meyer & Meyer-Hofmeister 1981; and also Lasota 2001, for an extensive review). A critical observational key test of the DIM is whether it can correctly predict the recurrence time and the observed peak and quiescent optical magnitudes of outbursting systems at known distances.

SS Cyg is one of the brightest and best-studied DN in the sky, reaching $V \simeq 8$ at peak outburst, and with a photometric record extending more than a century (e.g. Cannizzo 2012) and has therefore been used as a test case for the DIM. Bailey (1981)

Table 1. The 16 CVs and related objects from the catalogue of Ritter & Kolb which have a parallax measurement in the *Gaia* DR1 TGAS catalogue.

Source	$P_{\rm orb}$ (h)	Sub-type	*Gaia* parallax (mas)	Pre-*Gaia* parallax (mas)
Classical novae				
V603 Aql	3.32	N Aql 1918	2.92 ± 0.54	4.01 ± 0.14 (1)
RR Pic	3.48	N Pic 1925	2.45 ± 0.44	1.92 ± 0.18 (1)
HR Del	5.14	N Del 1967	0.99 ± 0.61	
Nova-like (NL)				
TT Ari	3.30	VY Scl	4.37 ± 0.42	
IX Vel	4.65	UX UMa	11.28 ± 0.26	10.4 ± 1.0 (2)
UX UMa	4.72	UX UMa	3.78 ± 0.28	
V3885 Sgr	4.97	UX UMa	7.38 ± 0.32	9.1 ± 2.0 (2)
Dwarf novae (DN)				
RX And	5.04	Z Cam	5.41 ± 0.55	
HL CMa	5.20	Z Cam	3.19 ± 0.28	
AH Her	6.19	Z Cam	3.02 ± 0.28	3.0 ± 1.5 (3)
SS Cyg	6.60	U Gem	8.56 ± 0.33	6.02 ± 0.46 (4)
				8.80 ± 0.12 (5)
				8.30 ± 0.41 (6)
				7.30 ± 0.20 (7)
Z Cam	6.96	Z Cam	4.56 ± 0.24	8.9 ± 1.7 (3)
BV Cen	14.64	U Gem	2.81 ± 0.38	
Magnetic				
AE Aqr	9.88	DQ Her	10.95 ± 0.26	9.8 ± 2.8 (2)
Others				
QU Car	10.90	Binary	2.28 ± 0.35	
V Sge	12.3	Binary	–0.35 ± 0.60	3.1 ± 13 (8)

Notes. We arrange them according to the CV sub-type, and include their orbital periods, parallax derived from DR1 (milli-arcsec) and previous parallax information where available.

References. (1) Harrison et al. (2013); (2) Duerbeck (1999); (3) Thorstensen (2003); (4) Harrison et al. (1999); (5) Miller-Jones et al. (2013); (6) Nelan & Bond (2013); (7) Harrison & McArthur (2016); (8) van Altena et al. (1995).

used the K-band magnitude (see Sect. 2) to determine a distance to SS Cyg of 95^{+18}_{-39} pc. Using the HST fine guidance sensor to measure its parallax, Harrison et al. (1999) determined a distance of 166 ± 12 pc. Schreiber & Gänsicke (2002) found that for this distance, the accretion disc limit cycle model (e.g. Cannizzo 1993) would imply a mean accretion rate too high to undergo outbursts. In other words, for a distance of 166 pc, SS Cyg should be a NL variable (see also Schreiber & Lasota 2007). The distance of SS Cyg has since then been subject to intense debate. Miller-Jones et al. (2013) obtained a VLBI parallax, which implied a distance of 114 ± 2 pc, consistent with the observed outburst properties in the DIM framework. The original HST data has been re-analysed several times, giving contradictory results (e.g. Nelan & Bond 2013; Harrison & McArthur 2016). However, only one of these results is consistent with the VLBI measurement (see Table 1).

The first *Gaia* release (DR1) on 2016 Sept. 14 included astrometric and photometric data of more than one billion stars, and parallax information for more than two million sources as a result of a joint *Tycho-Gaia* astrometric solution (TGAS, Gaia Collaboration 2016a). We cross-matched the TGAS catalogue with the Ritter & Kolb catalogue of CVs and related objects (Ritter & Kolb 2003, version 7.23, December 2015) and find 16 objects which are common to both (these are identified in Table 1). They have a range of orbital period between 3.3–14.6 h and a diversity of sub-type, with three classical novae which erupted in the early-mid 20th century (V603 Aql, RR Pic, HR Del); four NL variables (IX Vel, UX UMa, V3885 Sgr, and the VY Scl system TT Ari); six DN (SS Cyg, BV Cen, and the four Z Cam systems RX And, HL CMa, AH Her, and Z Cam); one magnetic CV (AE Aqr) and two systems that were claimed to be CVs, but are more likely massive binaries which may be interacting (QU Car, V Sge).

Since the current data release includes only bright ($V \lesssim 13$) stars, the sample is biased towards CVs with high accretion rates and long orbital periods. In this paper we outline their parallaxes and distances as determined from the *Gaia* DR1, and compare these with previous measurements. We also derive the absolute magnitudes of these systems making use of the AAVSO light curves and the TGAS distances, as well as their X-ray luminosities using fluxes from the literature or from unpublished *Swift* observations. Finally, we assess whether the mean mass accretion rates implied by the *Gaia* distances are consistent with the critical mass accretion rate as predicted by the DIM.

2. Determining distances to CVs and related objects

Since CVs show composite spectra, determining their distances has long been subject to substantial uncertainties. Early measurements relied on parallax determinations and proper motion studies for nearby bright CVs (e.g. Kraft & Luyten 1965). Only six CVs were included in the HIPPARCOS catalogue (Duerbeck 1999), and an additional small number of relatively accurate parallaxes were obtained using ground-based measurements (Thorstensen 2003, 2008).

Based on the fact that the overall contribution of the white dwarf and accretion disc to the overall brightness of the CV at infrared wavelengths is small compared to the secondary star, Bailey (1981) developed a method using the K-band magnitude which was insensitive to the evolutionary state and temperature of the secondary star. This method was further refined by Beuermann (2006) who made use of the surface brightness of the secondary star in selected TiO absorption bands. An independent estimate of the distance can be obtained for those CVs where the white dwarf dominates at ultraviolet wavelengths (e.g. Gänsicke et al. 2005), however, those estimates are limited by the unknown white dwarf mass, and hence radius (see Sect. 6).

Less precise estimates of CV distances are based on the expansion rate of the shell in classical novae (e.g. Cohen 1988) and on an empirical relationship between M_V at outburst and orbital period (Warner 1987, see also Patterson 2011). Distances to CVs have also been determined by comparing the linear polarisation of the CV with the distance-polarisation relationship (Barrett 1996) for nearby field stars (where the distances of the field stars are determined from photometry and spectral type).

3. Distances determined using *Gaia*

ESA's *Gaia* mission was launched in 2013 Dec with the goal to map the sky down to $g \sim 20.7$ measuring fundamental parameters such as position, photometry, parallax and proper motion of at least one billion stars (Gaia Collaboration 2016b). The *Gaia*

Table 2. Derived distances for the 16 CVs and related objects shown in Table 1.

Source	Pre-*Gaia* distance (pc)	*Gaia* distance (pc)	AAVSO Vis (mag)	M_V (mag)	X-ray luminosity (erg s^{-1})
Classical novae					
V603 Aql	249^{+9}_{-8} HST parallax (1)	328.3 ± 77.9	–0.5 → 11.7	–8.1 → 4.1	2.9×10^{32} (*Swift*)
RR Pic	521^{+54}_{-45} HST (1), 600 ± 60 expansion (2)	388.3 ± 87.8	1.0 → 12.2	–6.9 → 4.3	0.4×10^{31} (0.3–5 keV, *XMM*)
HR Del	970 ± 70 expansion (3)	560.7 ± 170.5	3.6 → 12.1	–5.1 → 3.4	1.5×10^{31} (*Swift*)
Nova-like					
TT Ari	335 ± 50 white dwarf/secondary (4)	228.8 ± 29.6	10.1 → 15.9	3.3 → 9.1	$6.4–131 \times 10^{30}$ (*Swift*)
IX Vel	96^{+10}_{-8} Hipp parallax (5)	88.8 ± 3.2	9.0 → 10.5	4.3 → 5.8	7.9×10^{30} (ASCA)
UX UMa	345 ± 34 colours/models (6)	263.5 ± 30.4	12.2 → 14.9	5.1 → 6.7	0.7×10^{31} (0.2–10 keV, *XMM*)
V3885 Sgr	110^{+30}_{-20} Hipp parallax (5)	135.9 ± 8.3	9.8 → 10.8	4.1 → 5.1	7.7×10^{30} (*Swift*)
Dwarf novae					
RX And	~200 spectra/models (7)	185.5 ± 23.7	10.1 → 15.6	3.8 → 9.3	$3.6–53 \times 10^{30}$ (*Swift*)
HL CMa	None	309.8 ± 42.7	10.6 → 14.9	3.1 → 7.4	$2.5–4.0 \times 10^{32}$ (*Swift*)
AH Her	660^{+270}_{-200} parallax (8)	325.0 ± 47.2	10.9 → 14.8	3.3 → 7.2	
SS Cyg	114 ± 2 VLA (9)	117.1 ± 6.2	8.0 → 12.7	2.6 → 7.4	$4.7–63 \times 10^{31}$ (*Swift*)
	121 ± 6, 166 ± 12 HST (10,11)				
Z Cam	163^{+68}_{-38} parallax (8)	219.3 ± 19.5	10.1 → 14.0	3.4 → 7.3	$8.1–18.4 \times 10^{30}$ (*Swift*)
BV Cen	~435 UV models (12)	344.3 ± 64.8	10.7 → 13.5	3.0 → 5.8	1.9×10^{32} (2–10 keV, *Suzaku*)
Magnetic					
AE Aqr	102^{+42}_{-23} parallax (8)	91.4 ± 3.3	10.6 → 12.2	5.8 → 7.4	7.5×10^{30} (*XMM Suzaku*)
Others					
QU Car	>500 (13)	410.2 ± 86.1	10.8 → 12.4	2.7 → 4.3	1.9×10^{32} (0.2–12 keV *XMM*)
V Sge	$320^{+\infty}_{-260}$ parallax (14)	761.5 ± 213.4	9.6 → 13.3	0.2 → 2.3	

Notes. The distances were taken from the catalogue of Astraatmadja & Bailer-Jones (2016) and we used the values for a scale length, $L = 0.11$ kpc. We also give the distance estimates prior to *Gaia* where available, the observed optical brightness range in the V-band determined from AAVSO data spanning the period 1995–2015 (apart from the three old novae), and the range in absolute magnitude M_V implied by the TGAS distances. We determine X-ray luminosities using the TGAS distance and X-ray flux compiled from the literature or from an analysis of *Swift* data.

References. (1) Harrison et al. (2013); (2) Gill & O'Brien (1998); (3) Harman & O'Brien (2003); (4) Gänsicke et al. (1999); (5) Duerbeck (1999); (6) Baptista et al. (1995); (7) Sion et al. (2001); (8) Thorstensen (2003); (9) Miller-Jones et al. (2013); (10) Nelan & Bond (2013); (11) Harrison et al. (1999); (12) Sion et al. (2007); (13) Gilliland & Philips (1982); (14) van Altena et al. (1995).

first data release DR1 uses data taken between 2014 July 25 and 2015 Sept. 16 (Gaia Collaboration 2016a, Lindegren et al. 2016), and provides G-band magnitudes and positions for 1.1 billion sources. For two million bright stars included in the *Tycho*-2 catalogue, parallaxes and proper motions are calculated using a joint *Tycho-Gaia* Astrometric Solution (TGAS). We list the *Gaia* parallaxes and uncertainties for 16 CVs and related objects which are in the TGAS catalogue in Table 1 together with previously determined parallaxes. We provide a short background summary of each source in Appendix A.

In the upper panel of Fig 1 we illustrate the parallaxes of sources shown in Table 1. For the reasons outlined in Sect. 1, the most keenly anticipated parallax of a CV was that of SS Cyg. We find that the *Gaia* parallax (8.56 ± 0.33 mas) is consistent with that determined using the VLA (8.80 ± 0.12 mas, Miller-Jones et al. 2013). However, it is consistent with only one of the HST parallax measurements (8.30 ± 0.41, Nelan & Bond 2013). There are HST parallaxes of two classical novae, V603 Aql and RR Pic, which are formally consistent with the *Gaia* parallexes at the 2σ and 1σ level respectively. The HIPPARCOS measurements of the NL systems IX Vel and V3885 Sgr are relatively high, but consistent with those of *Gaia* as are the ground based parallaxes of Thorstensen (2003).

For reasons outlined in Bailer-Jones (2015), obtaining distances and realistic uncertainties from parallaxes is not a trivial task (i.e. simply inverting the parallax from TGAS is not appropriate for systems with parallax uncertainties $\gtrsim$20%). Here, we make use of the distances and errors from the catalogue published by Astraatmadja & Bailer-Jones (2016), which require a choice of the scale length L. We compared the distances assuming $L = 0.11$ kpc and 1.35 kpc, and find that for sources closer than ~500 pc the distances and uncertainties are very similar. However, for more distant sources the distances and errors determined assuming $L = 1.35$ kpc start to become significantly larger compared to those determined assuming $L = 0.11$ kpc. In the following, we adopt the distance based on the choice of $L = 0.11$ kpc (which Astraatmadja & Bailer-Jones 2016 determined by fitting their Bayesian prior with the true distance distribution of stars included in a model of bright stars in the Milky Way). We list the derived *Gaia* distances and the pre-*Gaia* distances in Table 2, where we indicate whether the source's pre-*Gaia* distance was determined using a parallax measurement or through modelling of spectra or colours. We illustrate this comparison in Fig. 1.

We now make a more detailed comparison of the distances of the CVs and related objects in our sample with previous distance measurements. The distance and uncertainty to SS Cyg is virtually identical for the three scale lengths tabulated by Astraatmadja & Bailer-Jones (2016): 117.1±6.2 pc. This result is at odds with that of the most recent analysis of the HST derived parallax (137 ± 4 pc; Harrison & McArthur 2016). However, it is in excellent agreement with the parallax measurement using the VLBI (114 ± 2 pc; Miller-Jones et al. 2013) whose results were held up as a demonstration of the DIM being able to reproduce

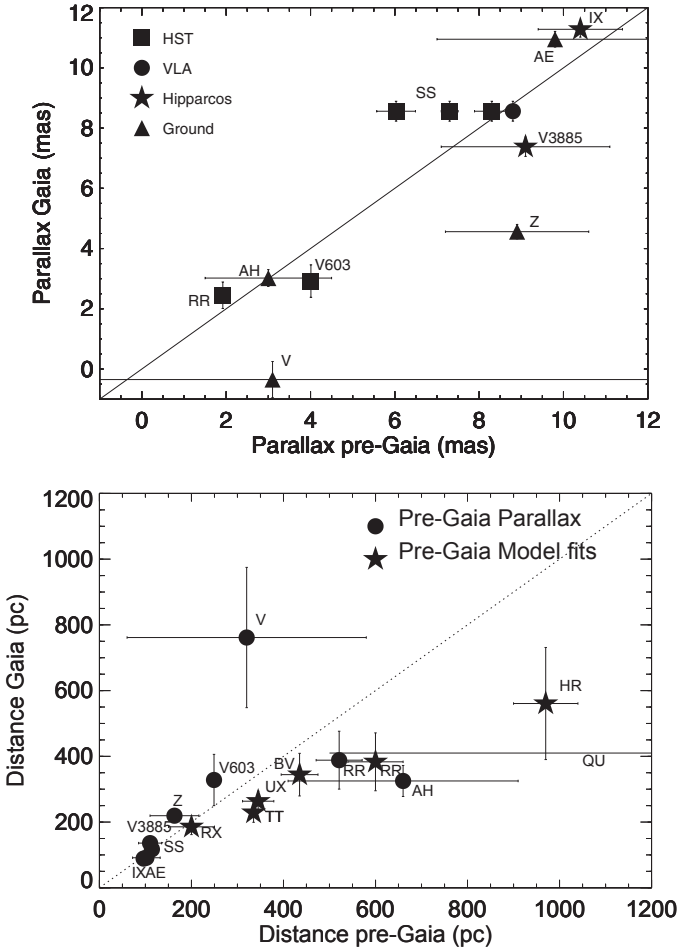

Fig. 1. *Upper panel*: parallaxes of sources which are in the TGAS catalogue and had previously determined parallaxes (the data measurements are outlined in Table 1). For SS Cyg there are four previous parallaxes. *Lower panel*: comparison of the distances of the 16 CVs in TGAS (taken from Astraatmadja & Bailer-Jones 2016, and tabulated in Table 2) with the best distance estimate pre-*Gaia*. We indicate by different symbols whether the pre-*Gaia* distance was determined via a parallax measurement or modelling spectra or colours. We note which system corresponds to which point by means of an abbreviation of the source name.

the optical outburst characteristics of this DN (see for example Schreiber & Gänsicke 2002). However, the apparent discrepancy of the various distance measurements meant that the question of whether the DIM was able to reproduce the characteristics of the long term light curve of SS Cyg (and hence of DN more generally) remained controversial. The HST study which is closest to (and consistent with) the *Gaia* distance is that of Nelan & Bond (2013) who found a distance of 120.5 ± 5.7 pc. We add in passing that Schreiber & Gänsicke (2002) note at the end of their paper that a distance of ∼117 pc would make the mass transfer rate derived from observations agree with the DIM. The *Gaia* distance to SS Cyg is 117.1 ± 6.2 pc and matches precisely with the prediction of the DIM. We show in Table 1 the parallax measurements derived by the groups discussed above.

Two other systems, the old novae V603 Aql, and RR Pic have HST parallaxes which imply a distance of 249^{+9}_{-8} pc and 521^{+54}_{-45} pc for V603 Aql and RR Pic respectively. As indicated previously, the errors on the *Gaia* distances are quite large and the distances derived using HST and *Gaia* are formally consistent. CVs with distances determined by HIPPARCOS (IX Vel, V3885 Sgr and AE Aqr) are consistent with the distances determined using *Gaia*. The very uncertain ground-based parallax of AH Her is consistent with, but now superseded by the lower, and much more accurate *Gaia* distance. For Z Cam, the best ground-based parallax is replaced by a somewhat larger *Gaia* distance. QU Car has a *Gaia* distance which is consistent with the lower limit previously found but not with the larger distance estimate of 2 kpc (Drew et al. 2003) and is therefore not as luminous as was once thought. With a distance of 760 pc the massive binary V Sge is the most luminous source under study here (with the exception of the old novae during their eruptions).

The other two old novae, RR Pic and HR Del, have distances determined using assumptions based on the expansion velocity, which are biased towards slightly greater distances compared to *Gaia* distances. For those objects whose distances were determined by fitting spectra or photometric colours, there is a slight bias for the *Gaia* distances being closer than the pre-*Gaia* estimates. In Appendix A we note the distances determined by Barrett (1996) for individual sources. In summary the distances to three NL systems are suprisingly consistent with the *Gaia* distances, although the distances to the classical novae are underestimated, and the distance to V Sge is grossly underestimated.

4. Absolute magnitude of outbursting CVs

We extracted the visual light curves of the 16 CVs in TGAS from the AAVSO[1] database (Kafka 2015) over the time interval 1995–2015, thereby ensuring the range of their variability is well characterised (we employed a light clipping to remove outlying points). The visual measurements generally well sample this 20 yr interval and we found fairly good agreement between visual measurements, and V-band CCD measurements which amateur astronomers were starting to use more commonly in the second half of this time period. We list in Table 1 the range in the visual magnitude for each source and the absolute magnitude computed using the TGAS distance (we do not account for interstellar extinction, but if $E_{B-V} = 0.03$, then M_V would be brighter by ∼0.1 mag).

In Fig. 2 we show M_V (max,min) for our targets as a function of orbital period. We also show the linear fits to outbursting sources as derived by Warner (1987) using those CVs which had known distances (Patterson 2011, shows a fit which is very similar to the Warner relationship). We find that the NL variables IX Vel and V3885 Sgr have $M_{V,\mathrm{max}}$ which are within ≃0.2 mag of the linear fit of Warner (1987). In contrast, TT Ari is ≃1.5 mag brighter and UX UMa is ≃0.7 mag fainter than this relationship implies. This may be due to an inclination effect since TT Ari has a low inclination (∼30°) making it appear brighter, whilst UX UMa has a high inclination (≃70°), making it fainter (see Patterson 2011, for a discussion on the relationship between M_V and binary inclination). The DN in our sample show no clear dependence on orbital period with a $M_{V,\mathrm{max}} \sim 3.2 \pm 0.4$, but we have a smaller sample, and a more restricted range in orbital period than the samples of Warner (1987) and Patterson (2011). The DN in our sample have a mean $M_{V,\mathrm{max}}$ which is ≃0.8 ± 0.4 mag brighter than predicted by the relationship of Warner (1987).

We also show the linear fits to $M_{V,\mathrm{min}}$ derived by Warner (1987) for outbursting systems in Fig. 2. As might be expected

[1] http://aavso.org

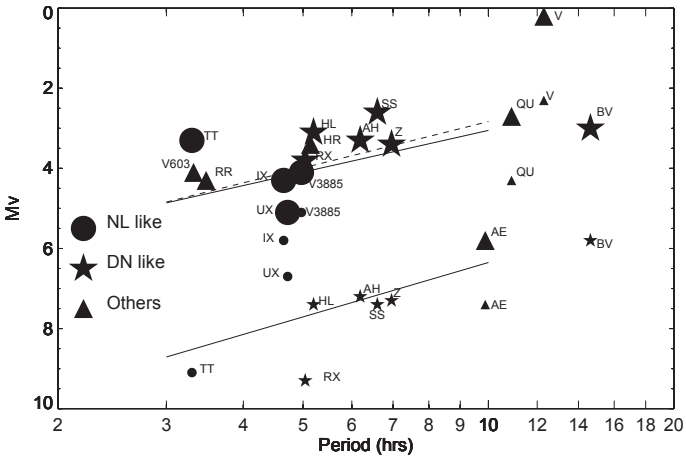

Fig. 2. Absolute magnitude for the maximum and minimum brightness for the sources in this study as a function of orbital period. We show the relationship of Warner (1987) for M_V at maximum and minimum where the smaller symbols indicate M_V minimum (the dashed line indicates the correlation determined by Patterson 2011). We note which system corresponds to which point by means of an abbreviation of the source name.

the NL systems (which do not show regular outbursts like the DN) show on average a $M_{V,\rm min}$ which is brighter by 1.5 ± 1.5 mag than expected from the Warner (1987) relationship. TT Ari shows dramatic dips in its long term light curve (hence the VY Scl sub-type). In contrast, DN are within 0.0 ± 0.7 mag of the $M_{V,\rm min}$ orbital period relationship. The one system which is discrepant is RX And which is 1.3 mag fainter than expected. RX And is an interesting system in that it appears to show evidence for both Z Cam and VY Scl behaviour making it fainter when undergoing a dip event (Schreiber et al. 2002).

We note that $M_{V,\rm min}$ for QU Car is consistent with Warner's linear relationship for outbursting CVs, while for V Sge $M_{V,\rm min}$ is ∼2 mag brighter than the CV trend. This indicates that V Sge is unlikely to be a CV, whilst the situation for QU Car is less clear. The magnetic CV AE Aqr has an $M_{V,\rm min}$ which is ∼1 mag fainter than the Warner (1987) fit for $M_{V,\rm min}$. This is not unexpected since it does not have a regular accretion disc (see the next section).

In Table 2 we also list the observed peak magnitude (taken from Strope et al. 2010) of the three old novae included in the TGAS catalogue and determine the outburst M_V (also given in Table 1) using the *Gaia* distances. We compare these absolute magnitudes with the predicted values using the nova calibration of Della Valle & Livio (1995), and the observables from Strope et al. (2010). The predicted values are $M_V = -8.9, -7.0$ and -6.8 for V603 Aql, RR Pic and HR Del, respectively, which compares with –8.1, –6.9 and –5.1 before accounting for extinction. Taking $E_{B-V} = 0.08, 0.0$ and 0.17 for V603 Aql, RR Pic and HR Del, respectively (Selvelli & Gilmozzi 2013), we obtain corrected absolute magnitudes of $M_V = -8.4$, –6.9 and –5.6. The observed magnitude of RR Pic is within 0.1 mag of the predicted magnitude, but V603 Aql and HR Del were 0.5 and 1.2 mag fainter than the nova decline calibration predicts. Given that the error on the *Gaia* distances to these three novae are 20–30 percent, we await more precise parallax measurements which will be available in DR2 before making definitive conclusions regarding the reliability of the nova distance calibrations.

5. X-ray luminosities

CVs typically exhibit strong X-ray emission that is seen to anti-correlate with the optical state of the disc (e.g. Mukai 2017). Observations over the outburst cycle of DN, for instance, show that X-ray emission is brightest during quiescence (e.g. Wheatley et al. 1996; Collins & Wheatley 2010; Fertig et al. 2011) and the X-rays are suppressed during the optical outburst where they are replaced by intense extreme ultraviolet emission (e.g. Wheatley et al. 2003). This behaviour means that X-ray luminosities measured with reliable distances can be used to assess the accretion state of the disc.

The X-rays are known to be emitted from very close to the white dwarf surface (e.g. Mukai et al. 1997; Wheatley & West 2003) and they are usually thought to arise in a narrow boundary layer between the accretion disc and white dwarf surface, where the kinetic energy of the disc material is thermalised. Indeed, unless the white dwarf is rotating very rapidly, this boundary layer is expected to emit half of the total accretion luminosity of the system (Pringle 1981). In order to explain some of the outburst properties of DN, however, it has also been suggested that the inner accretion disc may be eroded or truncated in low accretion rate systems (e.g. Livio & Pringle 1992; Meyer & Meyer-Hofmeister 1994; King 1997), in which case the X-ray emission could account for even more than half of the accretion luminosity in the low state.

The anti-correlation between X-rays and the optical state of the disc is usually interpreted as the response of the boundary layer to changing accretion rate (Pringle & Savonije 1979). At low accretion rates the boundary between disc and white dwarf will have low density and be optically thin to its own emission (whether it is a narrow boundary layer or a truncated inner disc region). It therefore cools inefficiently and emits thermal X-rays at high temperatures (Patterson & Raymond 1985a). In this state the X-ray luminosity can be used to trace the total accretion rate onto the white dwarf. At high accretion rates the density in the boundary region increases and it eventually becomes optically thick to its own emission, cooling to much lower temperatures despite its increase in total luminosity (Patterson & Raymond 1985b). In this state the luminosity is dominated by extreme-ultraviolet emission, which is difficult to use as a tracer of the accretion rate because it is strongly absorbed in the interstellar medium. However, the X-ray luminosity immediately prior to this transition can be used to determine the accretion rate at which the boundary layer becomes optically thick, at least in the case of SS Cyg (Wheatley et al. 2003).

The accretion rates of quiescent DN inferred from X-ray luminosities have been problematic for the DIM. This is because the X-ray luminosities are much higher than is consistent with a low-state disc extending down to the white dwarf surface (e.g. Lasota 2001; Wheatley et al. 2003) and because the accretion rates are seen to decrease rather than increase between outbursts (McGowan et al. 2004; Collins & Wheatley 2010; Fertig et al. 2011). These observations tend to support the suggestions that the inner disc is eroded in the low state.

Previous studies of X-ray luminosities based on parallax distances have found evidence for a weak correlation with orbital period (Baskill et al. 2005; Byckling et al. 2010). This suggests a correlation also with the long-term average accretion rate that is driven by the secular evolution of the system. Consistent with this, there is also a correlation between the quiescent X-ray luminosity and the outburst duty cycle, where duty cycle is defined as the proportion of time spent in outburst (Britt et al. 2015).

We have identified the X-ray flux of sources from the literature (see Appendix A for references) and determine their X-ray luminosity using the TGAS distance (Table 2). For a number of sources we have extracted the X-ray data from the *Swift* archive and extracted a mean X-ray spectrum, which we have fitted using an absorbed two-temperature thermal plasma model (Table 2 indicates which satellite has been used). In the interests of brevity we do not give details of the *Swift* observations here, but they have been reduced and analysed in an identical manner to that outlined for the study of the symbiotic nova AG Peg (Ramsay et al. 2016). In Table 2 we give the range in X-ray luminosity where there is more than one epoch of observation and illustrate this in Fig. 3 where we distinguish between the different classes of CV.

The maximum X-ray luminosities of DN, the old nova V603 Aql, and the nova-like TT Ari shown in Fig. 3 appear to define an upper bound to the X-ray luminosity that increases with orbital period from $L_X \sim 2 \times 10^{32}$ erg s^{-1} at 3 h to around $L_X \sim 6 \times 10^{32}$ erg s^{-1} at 7 h. This appears to provide further support for a correlation between quiescent accretion rate and the long-term average rate. For TT Ari this maximum X-ray luminosity corresponds to one of the dips in optical brightness to the quiescent disc state.

The other old novae (RR Pic and HR Del) and NL (together with TT Ari in its usual high state) all have lower X-ray luminosities that are in line with the dwarf novae in outburst. This indicates that the accretion discs in these novae and NL are in sustained high states, with high accretion rates onto the white dwarf and optically-thick boundary layers. It seems that there may also be a dependence of these high-state X-ray luminosities on orbital period, despite the considerable scatter seen in the dwarf novae (perhaps reflecting short-term variability).

AE Aqr has a low X-ray luminosity, similar to the high accretion rate states of short period systems, but it is believed to be in a highly unusual state in which most of the mass transfer flow from the secondary star is propelled away from the white dwarf by its rapidly rotating magnetic field (Wynn et al. 1997). Thus the low X-ray luminosity in this case is thought to reflect a low accretion rate onto the white dwarf rather than a high-state disc. The combination of faint absolute magnitude and low X-ray luminosity seems to be a strong indicator of the propelling state, and *Gaia* DR2 may allow other such systems to be identified.

QU Car has a high X-ray luminosity compared to other systems with high-state discs, with an X-ray luminosity comparable to quiescent DN. However, it has a much longer orbital period than the other systems, and its X-ray luminosity seems to be consistent with an extrapolation of the possible trend of increasing high-state luminosity with orbital period (as indicated by the lower dashed line in Fig. 3). This is a further indication that the X-ray luminosity of high accretion rate discs is correlated with the long-term average mass transfer rate, even though the total boundary layer luminosity is probably dominated by optically-thick emission in the extreme-ultraviolet.

Finally, we note that the reduced distance of SS Cyg has the effect of reducing the accretion rate at which the boundary later appears to be become optically-thick to its own emission from $1.0{\times}10^{16}$ g s^{-1} found by Wheatley et al. (2003) to $5.0{\times}10^{15}$ g s^{-1}, which is closer to that inferred for other systems by Fertig et al. (2011).

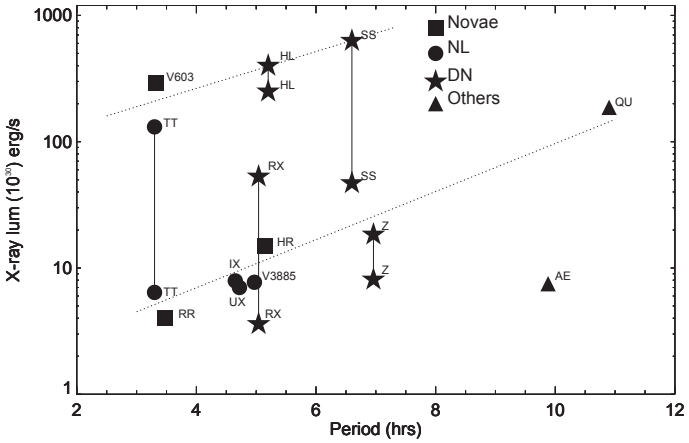

Fig. 3. X-ray luminosity of the 16 CVs in TGAS as a function of orbital period. For some systems we give the range of luminosity as quoted in the literature or measured from *Swift* data. We show different classes of CV with different symbols. The dotted lines illustrate how the X-ray luminosity appears to be related to the orbital period in high and low accretion states.

6. Implications for the white dwarf mass determinations

The accreting white dwarf dominates the ultraviolet emission of a significant number of CVs (e.g. Matteo & Szkody 1984) and model atmosphere fits to IUE, FUSE, and HST have resulted in measurements of the white dwarf effective temperatures of ≃75 CVs (Townsley & Gänsicke 2009; Pala et al. 2017), which provide constraints on the secular mean accretion rates (Townsley & Bildsten 2003). However, given that IUE and HST observations only cover a relatively small wavelength range, those measurements are subject to some degeneracy with the surface gravity, and hence the white dwarf mass. Accurate parallaxes break this degeneracy, as the flux scaling factor between the data and the model constrains the white dwarf mass, and via the use of a mass-radius relation (e.g. Panei et al. 2000), the surface gravity. Among the CVs in *Gaia* DR1 only TT Ari and RX And have white-dwarf dominated ultraviolet spectra.

Two IUE spectra were obtained during a prolonged low state of TT Ari in December 1982 and December 1983, which Gänsicke et al. (1999) modelled with a hot, $T_{\rm eff} \simeq 39\,000$ K, white dwarf. Adopting a very wide range for the white dwarf mass, $0.35 - 1.20\,M_\odot$, they concluded that the distance of TT Ari should be in the range of 125–385 pc. Using the *Gaia* measurement of ≃230 pc implies that the white dwarf mass is $\simeq 0.9\,M_\odot$, which is close to the mean mass of CV white dwarfs, $\langle M_{\rm wd} \rangle = 0.83 \pm 0.23\,M_\odot$ (Zorotovic et al. 2011). Unfortunately, the low quality of the IUE spectrum is now the limiting factor in the accuracy of the white dwarf parameters.

An HST spectrum of RX And was obtained during an unusual low state in December 1996, which Sion et al. (2001) modelled with a 34 000 K white dwarf. From the flux scaling factor, they estimated a distance of 200 pc for a $0.8\,M_\odot$ white dwarf, which is, within the uncertainties, consistent with the *Gaia* DR1 distance of 185.5 ± 23.7 pc. Taking the slightly lower DR1 distance value at face value would push the white dwarf mass up to $\simeq 0.9\,M_\odot$.

These two examples illustrate how accurate distances will help constrain CV white dwarf masses. The *Gaia* DR2 will not

only provide parallaxes to several dozen CVs which have high-quality ultraviolet observations, but also reduce the uncertainties in the parallax measurements, which will substantially increase the number of CV white dwarfs with accurate (≤10%) mass determinations.

7. Implications for the disc instability model

As briefly outlined in Sect. 1, the generally accepted model for DN outbursts is the DIM (Meyer & Meyer-Hofmeister 1981; Hameury et al. 1998). According to this model, DN outbursts are produced by a thermal and viscous instability that does not allow the disc to transport material inwards at the same rate as it receives it from the companion star. Instead, the disc has to switch between an excess of mass accretion, the so-called high state, and the quiescence state when matter accumulates in the disc as less mass is accreted than the disc receives from the secondary.

The DIM explains the observed characteristics of normal DN outbursts reasonably well. The DIM, however, also faces problems, for example, it seems to be difficult to reproduce irregular outbursts (e.g. Schreiber et al. 2002) and to explain the superoutbursts observed in SU UMa systems the DIM needs to be complemented either by a change in the mass transfer rate or a tidal instability (Osaki 1989; Smak 2004; Schreiber et al. 2004). Most of these problems are probably related to our limited understanding of the quiescence state (see Lasota 2001, for a review). In quiescence, matter must accumulate in the disc but it is uncertain at which radius this accumulation is most efficient. Also, as outlined in Sect. 5, quiescent X-ray luminosities are higher than predicted by the DIM, implying that more material is transported onto the white dwarf than expected. Together with the observed decrease in X-ray luminosity between outbursts, this suggests the inner disc is unexpectedly eroded during quiescence. It seems that the α viscosity prescription used in the DIM does not provide a good description of quiescence.

In contrast, the α formalism works well in the high state and the DIM makes clear and testable predictions. As the instability causing the outbursts is generated by the partial ionisation of hydrogen, one of the key predictions of the DIM is that above a certain mass transfer rate, the disc should be fully ionised and stable and no DN outbursts should occur. This critical mass transfer rate depends sensitively on the radius of the disc and the mass of the white dwarf. A frequently used prescription for the critical mass transfer rate is

$$\dot{M}_{\rm crit} = 9.5 \times 10^{15} R_{10}^{2.68} M_{\rm WD}^{-0.89} \ {\rm g/s}, \quad (1)$$

where $M_{\rm WD}$ is the white dwarf mass and R_{10} the disc radius in units of 10^{10} cm (Schreiber & Gänsicke 2002). NL variables and Z Cam stars during stand-still, and DN at the end of long outbursts should reach a quasi stationary state with a mass accretion rate $\sim\dot{M}_{\rm crit}$. During these quasi stationary states, the surface density and effective temperatures in the disc follow well-defined radial dependencies. In NL variables the disc must accrete at a rate exceeding the critical value and is expected to be in a quasi stationary state. At the end of a long DN outburst or during the stand-stills of Z Cam systems, the disc should be in the quasi stationary state with a mass accretion rate very similar to the critical rate. For a given set of system parameters, it is therefore possible to estimate the *absolute* brightness of a Z Cam disc during stand-still and from DN at the *end of long outbursts* as predicted by the DIM. For NL variables the brightness corresponding to the critical accretion rate represents a lower limit.

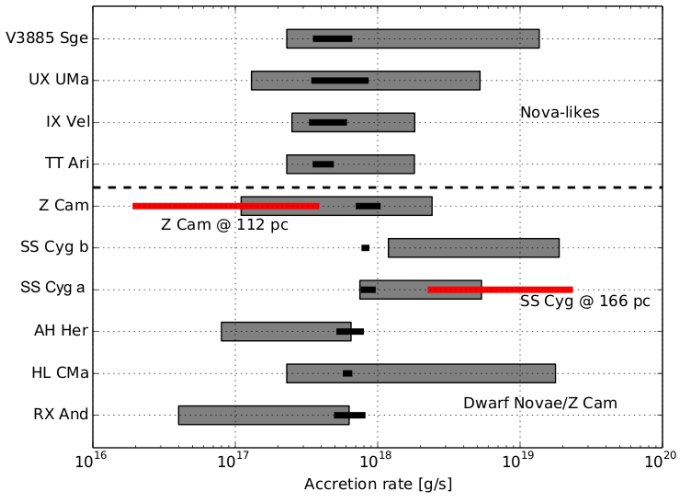

Fig. 4. Comparison of the mass accretion rates derived from observations (grey) and the critical mass accretion rate predicted by the DIM (black bars). In NL variables the DIM predicts the systems to accrete at a rate exceeding the critical one which is clearly possible as the grey bars extend to larger accretion rates than the black ones. For SS Cyg we tested the DIM prediction for two sets of parameters [a] and [b] and find agreement only if we use those derived by Friend et al. (1990) [a], which allow for a lower system inclination and a higher white dwarf mass. For Z Cam and SS Cyg we also show the accretion rates derived from the observations using the pre-*Gaia* distances (red bars) to demonstrate that the precise measurements now available brought into agreement theory and observations. The case of the two Z Cam stars AH Her and RX And is slightly worrying for the DIM as in both cases the overlap between both accretion rates is marginal.

These DIM predictions can be confronted with observations if the system parameters of a given CV and its distance are known reasonably well. We discussed the case of SS Cyg in Sect. 1, and noted that Schreiber & Gänsicke (2002) found strong disagreement between DIM predictions and a distance to SS Cyg of 166 pc as measured by Harrison et al. (1999). For agreement with the DIM, Schrieber & Gänsicke (2002) estimated a distance of ∼117 pc, in perfect agreement with the *Gaia* measurement.

In what follows we confront the DIM prediction with the *Gaia* distance measurements for nine CVs, that is, the four NL variables systems and five of the six DN. The long orbital period DN BV Cen does not qualify for the test as its outbursts are relatively short and the system never reaches the quasi stationary state. For the other nine systems we can assume a steady state accretion disc during high-states and calculate two mass transfer rates. First, we calculate the critical mass transfer rate as given by Eq. (1). This is straight forward and the main uncertainties involved are the white dwarf and secondary mass which together determine the disc radius which in the high-state should be close to the tidal truncation radius. Second, we calculate the accretion rate that is required to reproduce the observed absolute brightness assuming a steady state accretion disc. The uncertainties here are the stellar mass, inclination, observed brightness, and distance. We took into account all the uncertainties involved in the determination of both mass accretion rates. Thanks to the precise *Gaia* measurements, the uncertainties implied by the distances are minor. The dominating uncertainties are those of the system parameters which are notoriously difficult to measure in CVs with high mass transfer rates.

Table 3. System parameter and brightness values used for testing the predictions of the disc instability model.

Name	$M_{WD}[M_\odot]$	$M_2[M_\odot]$	Inc [degree]	m_V	Ref.
V3885 Sge	~0.7	~0.475	~65	9.5 ± 0.2	(1)
UX UMa	0.9 ± 0.3	0.39 ± 0.15	70 ± 5	13 ± 0.2	(2)
IX Vel	0.8 ± 0.2	0.52 ± 0.10	57 ± 2	9.5 ± 0.2	(3)
TT Ari	~0.9	~0.2	~30	10.8 ± 0.2	(4, 5)
Z Cam	0.99 ± 0.15	0.71 ± 0.10	57 ± 11	11.5 ± 0.2	(6)
SS Cyg [a]	1.19 ± 0.05	0.7 ± 0.1	37–53	8.6 ± 0.2	(7)
SS Cyg [b]	0.81 ± 0.2	0.55 ± 0.13	45–56	8.6 ± 0.2	(8)
AH Her	0.95 ± 0.1	0.76 ± 0.08	46 ± 3	12.5 ± 0.2	(9)
HL CMa	~0.83± 0.1	0.45 ± 0.1	~45	11.5 ± 0.2	(10)
RX And	1.14 ± 0.33	0.48 ± 0.03	51 ± 9	11.8 ± 0.2	(11)

Notes. The visual brightness is taken from the AAVSO light curve during stand-still of Z Cam stars and at the end of long outbursts for SS Cyg. At these phases the DIM predicts steady state accretion at rates close to the critical accretion rate. For the NL we used an average brightness. For HL CMa several parameters are completely unconstrained and we therefore used a broad range of inclinations (30–70 degrees) and the average WD mass for CVs of 0.83 ± 0.1. For SS Cyg we used two different sets of parameter [a] and [b]. If no error for the masses is given, we assumed an uncertainty of 0.1 $M_\odot$.

References. (1) Linnell et al. (2009); (2) Neustroev et al. (2011); (3) Linnell et al. (2007); (4) Gänsicke et al. (1999); (5) Wu et al. (2002); (6) Hartley et al. (2005a); (7) Friend et al. (1990); (8) Bitner et al. (2007); (9) Horne et al. (1986); (10) Hutchings et al. (1981); (11) Shafter (1983).

Figure 4 illustrates our results. The grey bars represent the accretion rates derived from observations using the parameters given in Table 3 while the DIM predictions are represented by the smaller black bars. The grey bars cover much larger ranges because of the uncertainty of the system parameters. For all NL variables in our sample, the *Gaia* distances lead to reasonable agreement with the DIM. The mass accretion rate derived from observations cover ranges largely exceeding the critical rate as required by the DIM. In the case of the Z Cam stars and the DN SS Cyg the situation is more complex and we therefore discuss each system individually.

For Z Cam itself the accretion rate we derived using the *Gaia* distance agrees perfectly with the DIM prediction, that is both accretion rates overlap. Interestingly, the pre-*Gaia* distance of 112 pc was in clear disagreement with the model (red bar in Fig. 4). If Z Cam was that close, the accretion rate during stand-still would be below the critical rate and the DIM would predict DN outbursts instead of a stand-still.

Surprisingly, the only pure DN in our sample, SS Cyg, is again causing some trouble. As mentioned above, the *Gaia* distance is in excellent agreement with the predictions made by Schreiber & Gänsicke (2002). However, back in 2002 we used the system parameters derived by Friend et al. (1990) which have been revised later by Bitner et al. (2007). According to the latter, the white dwarf in SS Cyg is less massive and the inclination higher than previously thought. Both these changes require a higher mass accretion rate to reproduce the same brightness. This higher mass accretion rate is in disagreement with the DIM as it significantly exceeds the critical value at the onset of the decline. In Fig. 4 we show the predicted mass accretion rate and the one derived from observations for both parameter sets. We also add a red bar which represent the mass accretion rate if SS Cyg was at 166 pc.

For HL CMa the observations agree reasonably well with the DIM prediction. The mass accretion rate derived from observations covers a large range of values as the inclination of the system is unknown. This large range includes the critical mass accretion rate and thus HL CMa might accrete during stand-still at a rate similar to or slightly larger than the critical one, as predicted by the DIM.

The situation is somewhat worrying for the remaining two systems of the Z Cam type, AH Her and RX And. Despite our conservative uncertainty estimates, the accretion rate derived from observations hardly reaches the critical mass accretion rate. The system parameters for both systems are too uncertain to call this a major problem of the DIM, but if the white dwarf masses can be confirmed to be relatively large and if the inclination does not greatly exceed the value given in Table 3, the model might face some serious problems.

8. Conclusions

The *Gaia* TGAS catalogue and the catalogue of Astraatmadja & Bailer-Jones (2016) provide parallaxes and distances to 16 CVs and related objects. The *Gaia* parallax to SS Cyg is consistent with that determined using a VLBI parallax measurement and is in spectacular agreement with the distance implied by the DIM when modelling the observed outburst behaviour of SS Cyg. The TGAS distances to CVs have allowed us tentatively to explore the relationship between absolute visual magnitude, accretion disc state and orbital period and how the sub-types of CVs relate. We have also shown that accurate X-ray luminosities allow the accretion state of the system to be determined, whether that be a high or low state accretion disc or a magnetic propeller, as well as determining the mass accretion rate in quiescence and at the transition to an optically-thick boundary layer in outburst. We have demonstrated the value of accurate parallaxes combined with ultraviolet observations in determining the mass of CV white dwarfs and the secular mass transfer rates, both key parameters in understanding the evolution of CVs. We have also estimated the critical mass accretion rate for the NL variables and the DN in our sample, and compared these values with the observational estimates of the mass accretion rates based on the *Gaia* distances and historic AAVSO data. We find good general agreement although it is somewhat marginal for a few systems. The second *Gaia* data release will provide parallaxes to many hundreds of CVs, and thus provide the data base necessary to extend these fundamental studies to CVs spanning the entire range of orbital period, mass transfer rate, and sub-type.

Acknowledgements. This work has made use of data from the European Space Agency (ESA) mission *Gaia* (https://www.cosmos.esa.int/gaia), processed by the *Gaia* Data Processing and Analysis Consortium (DPAC, https://www.cosmos.esa.int/web/gaia/dpac/consortium). Funding for the DPAC has been provided by national institutions, in particular the institutions participating in the *Gaia* Multilateral Agreement. We thank everyone who has been involved with the mission. We also thank the observers of the AAVSO for their tireless and important work. Armagh Observatory and Planetarium is core funded by the Northern Ireland Executive through the Dept for Communities. P.W. is supported by a STFC consolidated grant (ST/L000733/1). The research leading to these results has received funding from the European Research Council under the European Union's Seventh Framework Programme (FP/2007-2013)/ERC Grant Agreement No. 320964 (WDTracer). M.R.S. thanks for support from Fondecyt (grant 1141269). We thank the referee for a careful reading of the manuscript.

References

Astraatmadja, T. L., & Bailer-Jones, C. A. L. 2016, ApJ, 833, 119
Bailer-Jones, C. A. L. 2015, PASP, 127, 994
Bailey, J. 1981, MNRAS, 197, 31
Baptista, R., Horne, K., Hilditch, R. W., Mason, K. O., & Drew, J. E. 1995, ApJ, 448, 395
Barrett, P. 1996, PASP, 108, 412
Baskill, D. S., Wheatley, P. J., & Osborne, J. P. 2001, MNRAS, 328, 71
Baskill, D. S., Wheatley, P. J., & Osborne, J. P. 2005, MNRAS, 357, 626
Benedict, G. F., McArthur, B. E., Nelan, E. P., & Harrison T. E. 2017, PASP, 129, 2001
Beuermann, K. 2006, A&A, 460, 783
Bitner, M. A., Robinson, E. L., & Behr, B. B. 2007, ApJ, 662, 564
Britt, C. T., Maccarone, T., Pretorius, M. L., et al. 2015, MNRAS, 448, 3455
Byckling, K., Mukai, K., Thorstensen, J. R., & Osborne, J. P. 2010, MNRAS, 408, 2298
Cannizzo, J. K. 1993, ApJ, 419, 318
Cannizzo, J. K. 2012, ApJ, 757, 174
Cannizzo, J. K., & Mattei, J. A. 1992, ApJ, 401, 642
Chlebowski, T., Halpern, J. P., & Steiner, J. E. 1981, ApJ, 247, L35
Cohen, J. G. 1988, In The extragalactic distance scale; Proceedings of the ASP 100th Anniversary Symposium, Victoria, Canada, ASP Conf. Ser., 4, 114
Collins, D. J., & Wheatley, P. J. 2010, MNRAS, 402, 1816
Cordova, F. A., Mason, K. O., & Nelson, J. E. 1981, ApJ, 245, 609
Cowley, A. P., Crampton, D., Hutchings, J. B., & Marlborough, J. M. 1975, ApJ, 195, 413
Cowley, A. P., Crampton, D., & Hesser, J. E. 1977, ApJ, 214, 471
Della Valle, M., & Livio, M. 1995, ApJ, 452, 704
Done, C., & Osborne, J. P. 1997, MNRAS, 288, 649
Downes, R. A., & Duerbeck, H. W. 2000, AJ, 120, 2007
Drew, J. E., Hartley, L. E., Long, K. S., & van der Walt, J. 2003, MNRAS, 338, 401
Duerbeck, H. W. 1999, IBVS, 4731
Eracleous, M., Halpern, J., & Patterson, J. 1991, ApJ, 382, 290
Fertig, D., Mukai, K., Nelson, T., & Cannizzo, J. K. 2011, PASP, 123, 1054
Friedjung, M. 1997, New Astron., 2, 319
Friend, M. T., Martin, J. S., Connon-Smith, R., & Jones, D. H. P. 1990, MNRAS, 246, 654
Gaia Collaboration (Brown, A. G. A., et al.) 2016a, A&A, 595, A2
Gaia Collaboration (Prusti, T., et al.) 2016b, A&A, 595, A1
Gänsicke, B. T., Sion E. M., Beuermann, K., et al. 1999, A&A, 347, 178
Gänsicke, B. T., Szkody, P., Howell, S. B., & Sion, E. M. 2005, ApJ, 629, 451
Gänsicke, B. T., Dillon, M., Southworth, J., et al. 2009, MNRAS, 397, 2170
Garrison, R. F., Schild, R. E., Hiltner W. A., & Krzeminski W. 1984, ApJ, 276, L13
Gaposchkin, S. 1949, AJ, 54, 128
Gill, C. D., & O'Brien, T. J. 1998, MNRAS, 300, 221
Gilliland, R. L., & Philips, M. M. 1982, ApJ, 261, 617
Greiner, J., & van Teeseling, A. 1998, A&A, 339, L21
Hameury, J., Menou, K., Dubus, G., Lasota, J., & Hure, J. 1998, MNRAS, 298, 1048
Harman, D. J., & O'Brien, T. J. 2003, MNRAS, 344, 1219
Harrison, T. E., & McArthur, B. E. 2016, AAS Meeting, 227, 239.07
Harrison, T. E., McNamara, B. J., Szkody, P., et al. 1999, ApJ, 515, L93
Harrison, T. E., Johnson, J. J., & McArthur, B. E., et al. 2004, AJ, 127, 460
Harrison, T. E., Bornak, J., McArthur, B. E., & Benedict, G. F. 2013, ApJ, 767, 7
Hartley, L. E., Long, K. S., Froning, C. S., & Drew, J. E. 2005a, ApJ, 623, 425
Hartley, L. E., Murray, J. R., Drew, J. E., & Long, K. S. 2005b, MNRAS, 363, 285
Herbig, G. H., Preston, G. W., Smak, J., & Paczynski, B. 1965, ApJ, 141, 617
Hill, C. A., Watson, C. A., Shahbaz, T., Steeghs, D., & Dhillon, V. S. 2014, MNRAS, 444, 192
Horne, K., Wade, R. A., & Szkody, P. 1986, MNRAS, 219, 791
Hōshi R. 1979, Progr. Theor. Phys., 61, 1307
Hutchings, J. B. 1980, PASP, 92, 458
Hutchings, J. B., Cowley, A. P., Crampton, D., & Williams, G. 1981, PASP, 93, 741
Kafka, S. 2015, Observations from the AAVSO International Database, http://www.aavso.org
Kato, T. 2002, IBVS, 5243
King, A. R. 1997, MNRAS, 288, L16
Kitaguchi, T., An, H., Beloborodov, A. M., et al. 2014, ApJ, 782, 3
Knigge, C., Baraffe, I., & Patterson, J. 2011, ApJS, 194, 28
Kraft, R. P. 1962, ApJ, 135, 408
Kraft, R. P. 1964, ApJ, 139, 457
Kraft, R. P., & Luyten, W. J. 1965, ApJ, 142, 1041
Kraft, R. P., Krzemínski, W., & Mumford, G. S. 1969, ApJ, 158, 589
Kürster, M., & Barwig, H. 1988, A&A, 199, 201
Lasota, J.-P., 2001, New Astron., 45, 449
Lindegren, L., Lammers, U., Bastian, U., et al. 2016, A&A, 595, A4
Linnell, A. P., Godon, P., Hubeny, I., Sion, E. M., & Szkody, P. 2007, ApJ, 662, 1204
Linnell, A. P., Godon, P., Hubeny, I., et al. 2009, ApJ, 703, 1839
Livio, M., & Pringle, J. E., 1992, MNRAS, 259, L23
Lockley, J. J., Wood, J. H., Eyres, S. P. S., Naylor, T., & Shugarov, S. 1999, MNRAS, 310, 963
Johnson, C. B., Schaefer, B. E., Kroll, P., & Henden, A. A. 2014, ApJ, 780, L25
Matteo, M., & Szkody, P. 1984, AJ, 89, 863
Mayall, M. W. 1965, JRASC, 59, 285
McGowan, K. E., Priedhorsky, W. C., & Trudolyubov, S. P. 2004, ApJ, 601, 1100
Menzies, J. W., O'Donoghue, D., & Warner, B. 1986, Ap&SS, 122, 73
Meyer, F., & Meyer-Hofmeister, E. 1981, A&A, 104 L10
Meyer, F., & Meyer-Hofmeister, E. 1994, A&A, 288, 175
Miller-Jones, J. C. A., Sivakoff, G. R., Knigge, C., et al. 2013, Science, 340, 950
Moffat, A. F. J., & Shara, M. M. 1984, PASP, 96, 552
Mukai, K. 2017, PASP, 129, 062001
Mukai, K., & Orio, M. 2005, ApJ, 622, 602
Mukai, K., Wood, J. H., Naylor, T., Schlegel, E. M., & Swank, J. H. 1997, ApJ, 475, 812
Nelan, E. P., & Bond, H. E. 2013, ApJ, 773, L26
Neustroev, V. V., Suleimanov, V. F., Borisov, N. V., Belyakov, K. V., & Shearer, A. 2011, MNRAS, 410, 963
Osaki, Y. 1989, PASJ, 41, 1005
Pala, A., Gänsicke, B. T., Townsley, D., et al. 2017, MNRAS, 466, 2855
Panei, J. A., Althaus, L. G., & Benvenuto, O. G. 2000, A&A, 353, 970
Patterson, J. 1979, ApJ, 234, 978
Patterson, J. 2011, MNRAS, 411, 2695
Patterson, J., & Raymond, J. C. 1985a, ApJ, 292, 535
Patterson, J., & Raymond, J. C. 1985b, ApJ, 292, 550
Patterson, J., Thomas, G., Skillman, D. R., & Diaz, M. 1993, ApJS, 86, 235
Payne-Gaposchkin, C. 1969, ApJ, 158, 429
Pekon, Y., & Balman, S. 2008, MNRAS, 388, 921
Petit, M. 1960, Journal des Observateurs, 43, 17
Pratt, G. W., Mukai, K., Hassall, B. J. M., Naylor, T., & Wood, J. H. 2004, MNRAS, 348, L49
Pringle, J. E. 1981, ARA&A, 19, 137
Pringle, J. E., & Savonije, G. J. 1979, MNRAS, 187, 777
Ramsay, G., Sokoloski, J., Luna, G. J. M., & Nuñez, N. E. 2016, MNRAS, 461, 3599
Ribeiro, F. M. A., & Diaz, M. P. 2006, PASP, 118, 84
Ritter, H., & Kolb, U. 2003, A&A, 404, 301
Schreiber, M. R., & Gänsicke, B. T. 2002, A&A, 382, 124
Schreiber, M. R., & Lasota, J.-P. 2007, A&A, 473, 897
Schreiber, M. R., Gänsicke, B. T., & Mattei, J. A. 2002, A&A, 384, L6
Schreiber, M. R., Hameury, J.-M., & Lasota, J.-P. 2004, A&A, 427, 621
Selvelli, P., & Gilmozzi R. 2013, A&A, A49
Shafter, A. W. 1983, Ph.D., UCLA, USA
Shafter, A. W., Szkody P., Liebert J., et al. 1985, ApJ, 290, 707
Shara, M. M., Martin, C. D., Seibert, M. et al. 2007, Nature, 446, 159
Sion, E. M., Szkody, P., Gänsicke, B., et al. 2001, ApJ, 555, 834
Sion, E. M., Godon, P., Cheng, F., & Szkody, P. 2007, ApJ, 134, 886
Simonsen, M. 2011, JAVSO, 39, 66

Simonsen, M., Boyd, D., Goff, W., et al. 2014, JAVSO, 42, 177
Smak, J. 2004, Acta Astron., 54, 181
Still, M. D., Steeghs, D., Dhillon, V. S., & Buckley, D. A. H. 1999, MNRAS, 310, 39
Strope, R. J., Schaefer, B. E., & Henden, A. A. 2010, AJ, 140, 34
Thorstensen, J. R. 2003, AJ, 126, 3017
Thorstensen, J. R., Lépine, S., & Shara, M. 2008, AJ, 136, 2107
Townsley, D. M., & Bildsten, L. 2003, ApJ, 596, 227
Townsley, D. M., & Gänsicke, B. T. 2009, ApJ, 693, 1007
van Altena, W. F., Lee, J. T., & Hoffleit, E. D. 1995, The general catalogue of trigonometric stellar parallaxes, 4th edn. (New Haven, CT: Yale University Observatory)
van Teeseling, A., & Verbunt, F. 1994, A&A, 294, 519
van Teeseling, A., Beuermann, K., & Verbunt, F. 1996, A&A, 315, 467
Verbunt, F., Pringle, J. E., Wade, R. A., et al. 1984, MNRAS, 210, 197
Verbunt, F., Bunk, W. H., Ritter, H., & Pfeffermann, E. 1997, A&A, 327, 602
Vogt, N. 1975, A&A, 41, 15
Vogt, N., & Breysacher, J., 1980, ApJ, 235, 945
Walker, M. F., & Herbig, G. H. 1954, ApJ, 120, 278
Walker, M. F., & Chincarini, G. 1968, ApJ, 154, 157
Wargau, W., Drechsel, H., Rahe, J., & Bruch, A. 1983, MNRAS, 204, P35
Warner, B. 1987, MNRAS, 227, 23
Warner, B. 1995, Cataclysmic Variable Stars (Cambridge: Cambridge University Press)
Waterfield, W. F. H. 1929, Harvard Bull., 863, 6
Watson, C. A., Steeghs, D. Shahbaz, T., & Dhillon, V. S. 2007, MNRAS, 382, 1105
Wells, L. D. 1896, Harv. Coll. Obs. Circ., 12
Wheatley, P. J., & West, R. G. 2003, MNRAS, 345, 1009
Wheatley, P. J., Verbunt, F., Belloni, T., et al. 1996, A&A, 307, 137
Wheatley, P. J., Mauche, C. W., & Mattei, J. A. 2003, MNRAS, 345, 49
Wu, X., Li, Z., Ding, Y., Zhang, Z., & Li Zili 2002, ApJ, 569, 418
Wynn, G. A., King, A. R., & Horne, K. 1997, MNRAS, 286, 436
Xu, X.-J, Wang, Q. D., & Li, X.-D., 2016, ApJ, 818, 136
Zorotovic, M., Schreiber, M. R., & Gänsicke, B. T. 2011, A&A, 536, A42

Appendix A: Background notes on individual sources

V603 Aql: with a peak brightness of $V \sim 0.5$, Nova Aql 1918 (V603 Aql), is the brightest Galactic nova to ever have been identified (Strope et al. 2010). It took 20 yr for V603 Aql to fade to its pre-outburst brightness, but has continued to decline in brightness (Johnson et al. 2014). The astrometric distance determined using the HST fine guidance sensor is 249^{+9}_{-8} pc (Harrison et al. 2013) which compares with 328^{+60}_{-29} pc derived from nebular expansion studies (Downes & Duerbeck 2000). It has an orbital period of 3.3 h (Kraft 1964) and a low binary inclination ($i \sim 20°$, Patterson et al. 1993). Observations made using ASCA, RXTE and *Chandra* show flux variability which is likely caused by the changing maximum temperature of the plasma (Mukai & Orio 2005). A distance of 110 ± 6 pc is determined using linear polarisation (Barrett 1996). The distance obtained using *Gaia* is 328 ± 78 pc.

RR Pic: RR Pic was seen as a nova in 1925 reaching a peak of $V \sim 1.0$ and showed substantial variations in its brightness on the decline to quiescence of $V \sim 12.2$ (Strope et al. 2010). An orbital period of 3.48 h was identified by Vogt (1975) and the binary inclination is $60° < i < 80°$ (Riberio & Diaz 2006). RR Pic was observed using ROSAT and found to be a moderately bright X-ray source (van Teeseling et al. 1996) whilst observations made using *Chandra* show evidence for various emission lines in the X-ray spectrum (Pekon & Balman 2008). The astrometric distance determined using the HST fine guidance sensor is 521^{+54}_{-45} pc (Harrison et al. 2013). Using models of the expansion of the surrounding nebula, Gill & O'Brien (1998) estimate a distance to RR Pic of 600 ± 60 pc. A distance of 240 ± 65 pc is determined using linear polarisation (Barrett 1996). The distance obtained using *Gaia* is 388 ± 88 pc.

HR Del: HR Del was discovered as a nova in 1967 and had a peak brightness of $V \sim 3.6$ and returned to its quiescence mag $V \sim 12.1$ after about a decade (Strope et al. 2010). Kürster & Barwig (1988) determined an orbital period of 5.14 d and a binary inclination of $i \sim 40°$. Harman & O'Brien (2003) derived a distance of 970 ± 70 pc using models of the expansion of the nova shells. Although a strong UV source, HR Del was only marginally detected in hard X-rays using *EINSTEIN* (Hutchings 1980). The distance obtained using *Gaia* is 560 ± 170 pc.

TT Ari: TT Ari was one of the earliest CVs to be discovered and have its orbital period to be determined (3.3 h, Cowley et al. 1975). It was detected as a strong hard X-ray source using *Einstein* (Cordova et al. 1981). Further spectroscopic and photometric observations indicated it undergoes rapid fading events in the optical which are typical of VY Scl type CVs (Shafter et al 1985). Shafter et al. give a lower limit of 200 pc to its distance and find a relatively low binary inclination ($i \sim 30°$). Gänsicke et al. (1999) analysed IUE far-ultraviolet and optical spectroscopy obtained in 1982/83 during a deep low state, and detected the photospheric signatures of both the white dwarf and the M-dwarf companion. Based on the derived spectral type of the companion and the optical flux, they estimated a distance of $d = 335 \pm 50$ pc. A distance of 209 ± 64 pc is determined using linear polarisation (Barrett 1996). The distance obtained using *Gaia* is 228 ± 30 pc.

IX Vel: spectroscopic observations by Wargau et al. (1983) showed IX Vel to have spectra typical of a NL CV and giving a preliminary orbital period of 4.5 h. By fitting the *K*-band light curve Linnell et al. (2007) determined a binary inclination of 57±2°. No outbursts were detected over several years (Garrison et al. 1984) confirming IX Vel as a NL CV above the orbital period gap. Duerbeck (1999) gives a distance determined using HIPPARCOS of 96^{+10}_{-8} pc. X-ray observations of IX Vel made using ROSAT at two epochs show it as a strong X-ray source whilst further X-ray observations were made using ASCA (Baskill et al. 2005). A distance of 81 ± 44 pc is determined using linear polarisation (Barrett 1996). The distance obtained using *Gaia* is 89 ± 3 pc.

UX UMa: UX UMa is a bright ($V \sim 13$) eclipsing CV with an orbital period of 4.7 h (Walker & Herbig 1954) and is the archetypal member of the NL group of systems which are always in a high accretion state (Walker & Herbig 1954). Baptista et al. (1995) determine a distance of 345 ± 34 pc using photometric colours and estimates of the size of the accretion disc (Baptista et al. 1995) and derive a binary inclination of $i = 71.0° \pm 0.6°$. Observations made using *XMM-Newton* show that whilst there is no eclipse in soft X-rays there is an eclipse in hard X-rays indicating the latter are emitted in the boundary layer between the accretion disc and the white dwarf (Pratt et al. 2004). A distance of 333 ± 11 pc is determined using linear polarisation (Barrett 1996). The distance obtained using *Gaia* is 264 ± 30 pc.

V3885 Sgr: Cowley et al. (1977) identified V3885 Sgr as a bright ($V \sim 10.3$) CV which did not show outbursts. Hartley et al. (2005a) derived an orbital period of 5.0 h and detected spiral waves in the acretion disc, whilst its distance determined via HIPPARCOS data is 110^{+30}_{-20} pc (Duerbeck 1999). Linnell et al. (2009) determine a binary inclination of $i \sim 65°$ by modelling optical and UV spectra. van Teeseling & Verbunt (1994) showed V3885 Sgr to be moderately bright in ROSAT data and found that it showed a stable flux during these observations and in comparison with observations made using *EINSTEIN* and *EXOSAT*. The distance obtained using *Gaia* is 136 ± 8 pc.

RX And: RX And was discovered through regular optical outbursts and was found to be a binary with a period of 5.1 h by Kraft (1962). Observations made by members of the AAVSO show outbursts every few weeks, but also epochs where it is bright for several months (and typical of Z Cam stars) and epochs where it is faint for several months (and typical of VY Scl stars, Schreiber et al. 2002). Shafter (1983) determines a binary inclination of $i \sim 51 \pm 9°$ and Sion et al. (2001) determine a distance of 200 pc based on HST spectra and assumptions on the mass of the white dwarf. RX And was detected in X-rays using the *EINSTEIN* satellite (Eracleous et al. 1991) and as a weak source using ROSAT (Verbunt et al. (1997). A distance of 318 ± 55 pc is determined using linear polarisation (Barrett 1996). The distance obtained using *Gaia* is 185 ± 24 pc.

HL CMa: HL CMa showed outbursts approximately every 15 days (Chlebowski et al. 1981) although it can also show standstill events ($V \sim 12$) (Kato 2002). As such it appears to be a Z Cam type CV. Phase resolved spectroscopy made by Hutchings et al. (1981) showed an orbital period ~5 h and a binary inclination of $i \sim 45°$, with the orbital period being refined to 5.2 h (Still et al. 1999). A distance of 220 ± 10 pc is determined using linear polarisation (Barrett 1996). The distance obtained using *Gaia* is 310 ± 43 pc.

AH Her: AH Her was identified as a U Gem type-variable through its outbursts (Petit 1960) and has an orbital period of 5.9 h (Moffat & Shara 1984). The secondary star has an early to mid K spectral type, and has a binary inclination of $i \sim 46 \pm 3°$ (Horne et al. 1986). It has shown prolonged periods of standstill indicating it is Z Cam type CV (Simonsen 2011). Thorensten (2003) determined a distance of 660^{+270}_{-200} pc via parallax determinations. AH Her was detected in the ROSAT all-sky survey at a low rate (Verbunt et al. 1997). Simultaneous optical and UV (IUE) observations show that the UV flux follows the optical

during an outburst (Verbunt et al. 1984). A distance of 556 ± 110 pc is determined using linear polarisation (Barrett 1996). The distance obtained using *Gaia* is 325 ± 47 pc.

SS Cyg: SS Cyg is one of the best studied CVs in the sky being discovered in 1896 (Wells 1896) having an orbital period of 6.6 h (Walker & Chincarini 1968). It shows outbursts approximately every 50 days reaching a peak magnitude of $V \sim 8$ (Cannizzo & Mattei 1992). Friend et al. (1990) found a binary inclination of $i = 37°-53°$ assuming a white dwarf mass 0.55–1.2 $M_\odot$, while Bitner et al. (2007) find $i = 45°-56°$ and a white dwarf mass 0.81 ± 0.19 $M_\odot$. The distance to SS Cyg has been the subject of much debate. Using the HST fine guidance sensor to measure its parallax, Harrison et al. (2004) revised their previous distance to SS Cyg from 166 ± 12 pc to 152 ± 9 pc. Both distances were at odds with a parallax determined using the VLBI of 114 ± 2 pc (Miller-Jones et al. 2013). Although Nelan & Bond (2013) re-analysed the HST data and found a distance of 120.5 ± 5.7 pc, this analysis was questioned by Harrison & McArthur (2016) who concluded the distance to SS Cyg is 137 ± 4 pc (which remains at odds with the VLBI distance). Wheatley et al. (2003) shows that although there is a sudden burst of hard X-rays ∼1 d after the start of the optical outburst, they are suppressed shortly afterwards, only increasing again as the optical outburst approaches quiescence. A distance of 67 ± 17 pc is determined using linear polarisation (Barrett 1996). The distance obtained using *Gaia* is 117 ± 6 pc.

Z Cam: Z Cam is the prototype of CVs which normally show regular outbursts (similar to SS Cyg) but which show "standstills" which can last for many months (e.g. Mayall 1965). Z Cam stars have orbital periods longer than 3 h (Z Cam has an orbital period of 6.96 h, Kraft et al. 1969), placing them above the upper limit of the two to three hr period gap (Simonsen et al. 2014). Shafter (1983) determines a binary inclination of 57° ± 11°. The discovery of a shell of material around the binary implies a nova outburst in the distant past (Shara et al. 2007). Thorstensen (2003) determine a parallax of 163^{+68}_{-38} pc. Baskill et al. (2001) found using ASCA data that the observed flux was an order of magnitude higher at the point where it transitioned between quiescence and an outburst. The distance obtained using *Gaia* is 219 ± 20 pc.

BV Cen: BV Cen was found to show one magnitude variations on plates taken in 1928 (Waterfield 1929) and later classed as a U Gem type CV (Kraft & Luyten 1965). However, it was two decades later when the orbital period was shown to be 14.6 h which made it one of the longest period CVs (Vogt & Breysacher 1980). However, Menzies et al. (1986) show that BV Cen has a brighter absolute magnitude than expected for a regular DN and suggest it may have undergone a nova eruption. Watson et al. (2007) determine a binary orbital period of $i = 53° \pm 4°$. BV Cen was recently observed using *Suzaku* (Xu et al. 2016) and has a distance of 435 pc determined by modelling *FUSE* spectra (Sion et al. 2007). The distance obtained using *Gaia* is 344 ± 65 pc.

AE Aqr: AE Aqr has long been known as a bright variable, with Gaposchkin (1949) noting it was a member of the U Gem class. However, it was many years before its true nature was revealed, first when Payne-Gaposchkin (1969) identified the binary orbital period at 9.88 h and then when Patterson (1979) found evidence for a stable optical period of 33.08 s. The shorter period is due to the spin period of the accreting white dwarf and is classed as an intermediate polar, whose field strength is sufficiently high ($B \sim 1-10$ MG) to dominate the dynamics of the accretion flow at some distance from the white dwarf photosphere. The unique characteristics of this system led to an interpretation in which most of the mass transfer flow is propelled away from the white dwarf by its rapidly rotating magnetosphere (Wynn et al. 1997). Hill et al. (2014) determined a binary inclination of $i \sim 50°$. A distance of 102^{+42}_{-23} pc was determined using HIPPARCOS data (Friedjung 1997). Simultaneous observations were made of AE Aqr using NuStar and *Swift* in 2012 (Kitaguchi et al. 2014). A distance of 155 ± 55 pc is determined using linear polarisation (Barrett 1996). The distance obtained using *Gaia* is 91 ± 3 pc.

QU Car: spectroscopic observations showed that QU Car is a long period (10.9 h) binary with a hot accretion disc and a binary inclination $i < 60°$ (Gilliland & Philips 1982). The distance to QU Car is not well determined but Gilliland & Philips (1982) measured a distance >500 pc, whilst Drew et al. (2003) indicated it could lie at 2 kpc, which would make it a very luminous CV with a possible Carbon star secondary. QU Car was the target of two pointed observations by *XMM-Newton*. The distance obtained using *Gaia* is 410 ± 86 pc.

V Sge: V Sge is an eclipsing binary with a period of 12.3 h which shows epochs of a quasi-cycling behaviour when it can change its optical brightness by ∼3 mag on a timescale of weeks (Herbig et al. 1965). Its nature has been long debated but appears to consist of two hot stars, with the hotter star very close to filling its Roche lobe with a binary inclination of $i \sim 72°$ (Lockley et al. 1999). V Sge has a parallax distance of $320^{+\infty}_{-260}$ pc (van Altena et al. 1995). ROSAT observations showed that V Sge during a low optical states appears as a super-soft X-ray source (Greiner & van Teeseling 1998). A distance of 56 ± 56 pc is determined using linear polarisation (Barrett 1996). The distance obtained using *Gaia* is 760 ± 210 pc.